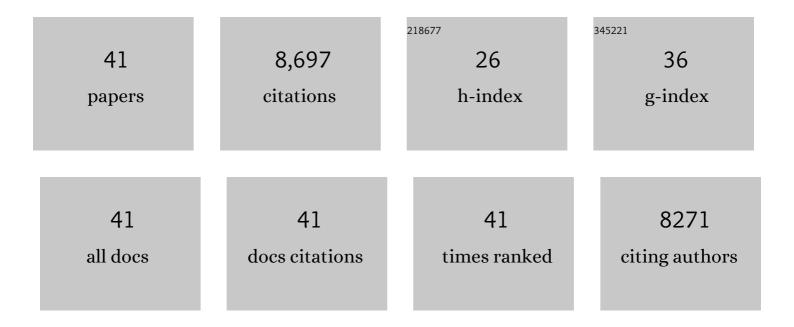
Qiaozhen Mu

List of Publications by Year in descending order

Source: https://exaly.com/author-pdf/11254812/publications.pdf Version: 2024-02-01



| # | Article | IF | CITATIONS |
|----|---|------|-----------|
| 1 | Improvements to a MODIS global terrestrial evapotranspiration algorithm. Remote Sensing of Environment, 2011, 115, 1781-1800. | 11.0 | 2,025 |
| 2 | Recent decline in the global land evapotranspiration trend due to limited moisture supply. Nature, 2010, 467, 951-954. | 27.8 | 1,771 |
| 3 | Development of a global evapotranspiration algorithm based on MODIS and global meteorology data. Remote Sensing of Environment, 2007, 111, 519-536. | 11.0 | 1,349 |
| 4 | Regional evaporation estimates from flux tower and MODIS satellite data. Remote Sensing of Environment, 2007, 106, 285-304. | 11.0 | 623 |
| 5 | Local cooling and warming effects of forests based on satellite observations. Nature Communications, 2015, 6, 6603. | 12.8 | 392 |
| 6 | A Remotely Sensed Global Terrestrial Drought Severity Index. Bulletin of the American Meteorological Society, 2013, 94, 83-98. | 3.3 | 351 |
| 7 | Comparison of satellite-based evapotranspiration models over terrestrial ecosystems in China. Remote Sensing of Environment, 2014, 140, 279-293. | 11.0 | 217 |
| 8 | Satellite based analysis of northern ET trends and associated changes in the regional water balance from 1983 to 2005. Journal of Hydrology, 2009, 379, 92-110. | 5.4 | 212 |
| 9 | Direct impacts on local climate of sugar-cane expansion in Brazil. Nature Climate Change, 2011, 1, 105-109. | 18.8 | 208 |
| 10 | Validation of MODIS 16 global terrestrial evapotranspiration products in various climates and land cover types in Asia. KSCE Journal of Civil Engineering, 2012, 16, 229-238. | 1.9 | 168 |
| 11 | Upscaling key ecosystem functions across the conterminous United States by a water-centric ecosystem model. Journal of Geophysical Research, 2011, 116, . | 3.3 | 159 |
| 12 | Bayesian multimodel estimation of global terrestrial latent heat flux from eddy covariance, meteorological, and satellite observations. Journal of Geophysical Research D: Atmospheres, 2014, 119, 4521-4545. | 3.3 | 146 |
| 13 | Potential and Actual impacts of deforestation and afforestation on land surface temperature. Journal of Geophysical Research D: Atmospheres, 2016, 121, 14,372. | 3.3 | 112 |
| 14 | Assessing the remotely sensed Drought Severity Index for agricultural drought monitoring and impact analysis in North China. Ecological Indicators, 2016, 63, 296-309. | 6.3 | 111 |
| 15 | Evaluating water stress controls on primary production in biogeochemical and remote sensing based models. Journal of Geophysical Research, 2007, 112, . | 3.3 | 108 |
| 16 | Improving global terrestrial evapotranspiration estimation using support vector machine by integrating three process-based algorithms. Agricultural and Forest Meteorology, 2017, 242, 55-74. | 4.8 | 96 |
| 17 | A satellite-based hybrid algorithm to determine the Priestley–Taylor parameter for global terrestrial latent heat flux estimation across multiple biomes. Remote Sensing of Environment, 2015, 165, 216-233. | 11.0 | 92 |
| 18 | Comparing Evapotranspiration from Eddy Covariance Measurements, Water Budgets, Remote Sensing, and Land Surface Models over Canadaa,b. Journal of Hydrometeorology, 2015, 16, 1540-1560. | 1.9 | 75 |

Qiaozhen Mu

| # | Article | IF | CITATIONS |
|----|--|------|-----------|
| 19 | Satellite assessment of land surface evapotranspiration for the panâ€Arctic domain. Water Resources Research, 2009, 45, . | 4.2 | 74 |
| 20 | The net carbon drawdown of small scale afforestation from satellite observations. Global and Planetary Change, 2009, 69, 195-204. | 3.5 | 56 |
| 21 | Evaluation of NLDASâ€2 evapotranspiration against tower flux site observations. Hydrological Processes, 2015, 29, 1757-1771. | 2.6 | 49 |
| 22 | Multi-sensor model-data fusion for estimation of hydrologic and energy flux parameters. Remote Sensing of Environment, 2008, 112, 1306-1319. | 11.0 | 48 |
| 23 | Contribution of increasing CO ₂ and climate change to the carbon cycle in China's ecosystems. Journal of Geophysical Research, 2008, 113, . | 3.3 | 46 |
| 24 | Satelliteâ€derived estimates of forest leaf area index in southwest Western Australia are not tightly coupled to interannual variations in rainfall: implications for groundwater decline in a drying climate. Global Change Biology, 2013, 19, 2401-2412. | 9.5 | 41 |
| 25 | Evolution of hydrological and carbon cycles under a changing climate. Hydrological Processes, 2011, 25, 4093-4102. | 2.6 | 34 |
| 26 | MODIS Reflective Solar Bands On-Orbit Calibration and Performance. IEEE Transactions on Geoscience and Remote Sensing, 2019, 57, 6355-6371. | 6.3 | 33 |
| 27 | Optimization of a Deep Convective Cloud Technique in Evaluating the Long-Term Radiometric Stability of MODIS Reflective Solar Bands. Remote Sensing, 2017, 9, 535. | 4.0 | 23 |
| 28 | VIIRS Reflective Solar Band Radiometric and Stability Evaluation Using Deep Convective Clouds. IEEE Transactions on Geoscience and Remote Sensing, 2016, 54, 7009-7017. | 6.3 | 14 |
| 29 | Assessment of MODIS RSB detector uniformity using deep convective clouds. Journal of Geophysical Research D: Atmospheres, 2016, 121, 4783-4796. | 3.3 | 11 |
| 30 | Results From the Deep Convective Clouds-Based Response Versus Scan-Angle Characterization for the MODIS Reflective Solar Bands. IEEE Transactions on Geoscience and Remote Sensing, 2018, 56, 1115-1128. | 6.3 | 10 |
| 31 | Exploring the stability and residual response versus scan angle effects in SNPP VIIRS sensor data record reflectance products using deep convective clouds. Journal of Applied Remote Sensing, 2018, 12, 1. | 1.3 | 8 |
| 32 | Global-Scale Estimation of Land Surface Heat Fluxes from Space. , 2013, , 249-282. | | 5 |
| 33 | Positional Dependence of SNPP VIIRS Solar Diffuser BRDF Change Factor: An Empirical Approach. IEEE Transactions on Geoscience and Remote Sensing, 2021, 59, 8056-8061. | 6.3 | 5 |
| 34 | Using MODIS weekly evapotranspiration to monitor drought. Proceedings of SPIE, 2016, , . | 0.8 | 5 |
| 35 | Assessment of SNPP VIIRS RSB detector-to-detector differences using deep convective clouds and deserts. Journal of Applied Remote Sensing, 2020, 14, 1. | 1.3 | 5 |
| 36 | Characterization of the on-orbit response versus scan angle for Terra MODIS SWIR bands in Collection 7. Journal of Applied Remote Sensing, 2022, 16, . | 1.3 | 4 |

QIAOZHEN MU

| # | Article | IF | CITATIONS |
|----|---|-----|-----------|
| 37 | Assessment of MODIS on-orbit calibration using a deep convective cloud technique. Proceedings of SPIE, 2016, , . | 0.8 | 3 |
| 38 | Assessment of Terra MODIS thermal emissive band calibration using cold targets and measurements in lunar roll events. , 2018, , . | | 3 |
| 39 | Evaluating the long-term stability and response versus scan angle effect in the SNPP VIIRS SDR reflectance product using a deep convective cloud technique. , 2018, , . | | 3 |
| 40 | Remote Sensing and Modeling of Global Evapotranspiration. , 2012, , 443-480. | | 1 |
| 41 | MODIS detector differences using deep convective clouds and desert targets. , 2020, , . | | 1 |
| | | | |